Clim. Past Discuss., 6, 2005–2054, 2010
www.clim-past-discuss.net/6/2005/2010/
doi:10.5194/cpd-6-2005-2010

Climate of the Past Discussions

Modeling Mediterranean ocean climate of the Last Glacial Maximum

U. Mikolajewicz

Max-Planck-Institut für Meteorologie, Bundesstr. 53, 20146 Hamburg, Germany

Received: 25 August 2010 – Accepted: 5 September 2010 – Published: 1 October 2010

Correspondence to: U. Mikolajewicz (uwe.mikolajewicz@zmaw.de)

Published by Copernicus Publications on behalf of the European Geosciences Union.

Modeling Mediterranean ocean climate of the LGM

U. Mikolajewicz

Abstract

A regional ocean general circulation model of the Mediterranean is used to study the climate of the last glacial maximum. The atmospheric forcing for these simulations has been derived from simulations with an atmospheric general circulation model, which in turn was forced with surface conditions from a coarse resolution earth system model. The model is successful in reproducing the general patterns of reconstructed sea surface temperature anomalies with the strongest cooling in summer in the northwestern Mediterranean and weak cooling in the Levantine, although the model underestimates the extent of the summer cooling in the western Mediterranean. However, there is a strong vertical gradient associated with this pattern of summer cooling, which makes the comparison with reconstructions nontrivial. The exchange with the Atlantic is decreased to roughly one half of its present value, which can be explained by the shallower Strait of Gibraltar as a consequence of lower global sea level. This reduced exchange causes a strong increase of the salinity in the Mediterranean in spite of reduced net evaporation.

1 Introduction

The Mediterranean is a semi-enclosed basin connected with the Atlantic by the narrow and shallow Strait of Gibraltar. It is an evaporative basin characterized by an anti-estuarine circulation with active deep water formation. It is influenced by both the monsoon circulation as well as the European climate.

The last glacial maximum (LGM) around 21 kyr BP is a well studied time slice with a glacial climate substantially different from present climate. The first regional reconstruction of LGM sea surface temperature (SST) from assemblages of foraminifera in the Mediterranean (Thiede, 1978) showed a marked difference in the cooling between eastern and western Mediterranean: The cooling in the northwestern Mediterranean was much stronger than in the eastern Mediterranean. Thiede (1978) also showed the

CPD
6, 2005–2054, 2010
Modeling Mediterranean ocean climate of the LGM
U. Mikolajewicz

presence of a cool fresh tongue in the Levantine originating from the Aegean. A recent reconstruction (Hayes et al., 2005) essentially confirmed the strong gradient in the climate signal between eastern and western Mediterranean, but did not find the cold fresh tongue. They found the strongest cooling in the northwestern Mediterranean in summer, whereas the cooling in the Levantine was small. Temperature estimates from alkenone unsaturation, however, indicate quite strong cooling (approx. 10 K) in the eastern Mediterranean (e.g. Emeis et al., 2003; Almogi-Labin et al., 2009), which conflicts with the weak cooling reported from assemblages of foraminifera. A comprehensive overview over the knowledge about the state of the Mediterranean at LGM can be found in Robinson et al. (2006).

Due to the lower sea level, the sill depth of the Strait of Gibraltar was reduced at LGM. This would under the assumption of hydraulic control result in reduced exchange rates between Atlantic and Mediterranean (e.g. Bryden and Stommel, 1984; Rohling and Bryden, 1994), which in turn would lead to higher salinity in the Mediterranean, which is consistent with geological evidence (e.g. Thunell and Williams, 1989).

Although the Mediterranean is an almost ideal region for regional ocean modeling due to the very limited exchange with the Atlantic, only very few attempts have been made to simulate the glacial circulation. Bigg (1994) used a regional ocean model forced with surface fluxes calculated interactively from bulk formulas with atmospheric input data derived from simulations with a coarse-resolution atmosphere-only model. His results suffered from short-comings of the atmospheric forcing and his ocean climate. Whereas this approach led to a substantial cooler climate, the effect on salinity was rather small, which might be an artifact due the short simulation period.

Myers et al. (1998) used a regional ocean general circulation model (GCM) with a rather realistic climate to investigate changes in deep water and ocean circulation. Their approach to LGM surface forcing was completely different than Bigg's (1994) approach: They imposed SST and sea surface salinity (SSS) anomalies derived from reconstructions onto their climatological present days SST and SST forcing, which was used for restoring. Their prescribed salinity anomalies were always strongest in the eastern Levantine. Their model responded to these changes in thermohaline forcing with an eastward shift of the deep water formation in the eastern basin from the Adriatic to the Rhodes gyre. In the western basin the location of deep water formation did not change substantially.

The model study presented here follows a similar approach as the study of Bigg (1994). A regional ocean model is forced with atmospheric input data from high-resolution atmospheric model simulations. River input and Atlantic hydrography are modified as well according to model results. Except from the ice sheet extent, the atmospheric composition and global sea level, no reconstructions enter the model. This method has the advantage that the model results are completely independent from e.g. SST reconstructions, which allows to use these data for the validation of the model results.

The goal of this study is to investigate with a dynamical downscaling approach the mechanisms which are responsible for the strong east-west gradient in summer cooling. Another focus of this paper is to model the associated changes in ocean circulation. In Sect. 2 of this paper the model and forcing are described. The climate of the control run is described and compared to observational estimates in Sect. 3. The setup for the LGM is described in Sect. 4 and the results for this time slice in Sect. 5.

2 Model and forcing

The model used in this study is a regional version of the primitive equation ocean general circulation model MPIOM (Max-Planck-Institute ocean model, Maier-Reimer, 1997; Marsland, 2003). The model covers the entire Mediterranean, the Black Sea and a small Atlantic box with a mean horizontal resolution of 20 km and is eddy-permitting. The topography of the model is shown in Fig. 1. The model has 29 unevenly spaced vertical levels, 8 of them in the top 100 m, and uses partial cells at the bottom. The model has a free surface. At the western margin of the Atlantic box a sponge zone with a restoring of temperature and salinity towards monthly climatological hydrography is used in order to prescribe the properties of the inflowing Atlantic water.

Heat fluxes at the surface are calculated using standard bulk-formulas with prescribed atmospheric forcing values and model SST. Prescribed input parameters are daily values of near-surface air temperature, dew point temperature, wind speed and downward radiative fluxes (shortwave and longwave). The upward longwave radiation is calculated from the model SST. The penetration of shortwave radiation into the ocean is set according to Jerlov optical water types Ib in the Mediterranean and III in the Black Sea (Jerlov, 1976).

Freshwater fluxes are calculated from prescribed daily precipitation and monthly climatological river runoff. Evaporation is calculated from the interactively calculated latent heat fluxes. The model uses a mass flux boundary condition for freshwater fluxes. As the Mediterranean is an evaporative basin, sea level would sink continuously. This is accounted for by weakly restoring the sea level at the westernmost grid points of the Atlantic box towards zero. Wind stress is prescribed directly.

The atmospheric forcing has been derived from time slice simulations with the atmospheric general circulation model ECHAM5 (Roeckner et al., 2003). The spectral model has been run in a horizontal resolution of T106 (approximately 1.125 °resolution on a Gaussian grid) with 39 vertical levels. SST, sea ice and vegetation distribution were derived from steady state simulations with a coarse resolution earth system model (ESM, Mikolajewicz et al., 2007). SSTs were corrected for systematic biases. Details of the procedure can be found in Arpe et al. (2010).

Two simulations were carried out (Arpe et al., 2010). One simulation represents a preindustrial climate (insolation corresponding to 1950, atmospheric partial pressure of CO_2 of 280 ppm) with present topography and glacier distribution. The other simulation represents the state of the LGM with topography and ice sheet according to the ICE-5G reconstruction (Peltier, 2004). Other important modifications include insolation (according to 21 kyrBP) and atmospheric composition ($p\mathrm{CO}_2$ of 185 ppm). The simulations closely follow the PMIP2 protocol (Braconnot et al., 2007).

CPD
6, 2005–2054, 2010

From these simulations, 20 years of daily atmospheric forcing were derived for each experiment through bilinear interpolation of atmospheric data from ocean grid points onto the grid of the ocean model. The forcing thus contains daily and interannual variability and it is applied repetitively. A monthly river runoff climatology was derived from these simulations using a hydrological discharge model (Hagemann and Dümenil-Gates, 2003). The model used river masks adapted to the respective topographies for the two time slices. For the Mediterranean, however, these changes were basically restricted to regions like the Adriatic, where the coastline strongly differed due to to lower global sea level.

Compared with observations, this approach leads to a strong overestimation of the Nile discharge. The main causes for this are an overestimation of the precipitation in the source regions of the Nile as well as the neglect of evaporation from the rivers during their way towards the Mediterranean Sea. Once the surface module of the atmospheric model has calculated a runoff (either surface or deep drainage), it is transferred to the hydrological discharge model. The model transfers the discharge to the coast, but a evaporative loss is not permitted. Thus the calculated runoff of the Nile is $9700\,m^3 s^{-1}$. Ludwig et al. (2009) report that more than half of the water generated by surface runoff is lost. Only approximately 40% of the water reach Aswan. The observed runoff from the Nile prior to the Aswan Dam is $2900\,m^3 s^{-1}$ (calculated from Vörösmarty et al., 1998). However, as this value also represents some effects of irrigation, it was decided to use a simple correction of 50% for the purpose of this study. For consistency, this correction was applied in the LGM simulation as well.

All simulations were started from homogeneous water with 38‰ and 20 °C. For the Black Sea an initial salinity of 20‰ was used. A model initialization with relative light homogeneous water has the advantage compared to initialization with climatology that it guarantees that all the water masses found in the model have been produced by the model and are not remains of the initial conditions. During the spin up minor corrections were made in the parameterizations, e.g. the first 99 years of the simulations were run with the full Nile discharge. However, all simulations have been run at least 500 years without any changes. The length of the simulations was different, the glacial simulations generally needed longer to reach a steady state due to the longer turnover times for the glacial Mediterranean. Figures shown in this paper represent an average over the last 100 years of the simulations.

3 Climate of the control simulation

The approach used here is, with a few exceptions, based on modeled input data. The comparison of the simulated model climate with observed ocean climate allows to assess both the quality of the model and of the model forcing. The deviations of CTL climate from the observed state of the Mediterranean yield at least a rough estimate of the quality of the simulated LGM climate. This would not have been possible, if only anomalies would have been used. The general approach is essentially similar to the approach of Bigg (1994). Bigg (1994), however, used much coarser models, both for the ocean as well as for the atmospheric model, which they used to derive the atmospheric forcing for their ocean model.

For the control simulation CTL, the model was integrated for 1299 years with the forcing derived from the preindustrial present day simulation of the atmospheric GCM. The remaining drift for the Mediterranean at 2029 m depth is 0.003 K/century for temperature and 0.002 ‰/century for salinity. The drift in surface salinity is 0.0002 ‰/century. The drift in the Black Sea towards higher salinity is still substantial: 0.07 ‰/century at the surface and 0.1 ‰/century at 1401 m depth.

This section deals with the assessment of the ability of the model to simulate some key parameters of the Mediterranean ocean climate, when driven with a forcing derived from the present day preindustrial simulation of the atmosphere model. This simulation will in the following be used as control simulation CTL for the LGM simulation. It is assumed here that the potential effect of anthropogenic climate change on the Mediterranean ocean climate, as represented in e.g. the climatology (Medar, 2002, henceforth MEDATLAS), is small and that the effect can be neglected.

In Fig. 2 the differences between modeled and observed SSTs are shown. With a few exceptions, the modeled open ocean winter (JFM) and summer (JAS) SSTs are close to observations with a typical error smaller than 1 K. In the model, SST refers to the temperature of the uppermost layer, which has a thickness of 12 m plus sea level. For consistency the observations have been linearly interpolated onto 6 m depth, the center of the uppermost model level.

In winter (JFM), the model shows a cold bias in the Levantine and Ionian Seas. SST errors in excess of 1 K are simulated in the northern edge of the Adriatic, southwest of Cyprus and in small regions south of Crete. In summer, the model produces too warm temperatures around the Strait of Gibraltar. This is probably an effect of the neglect of tides, which substantially would enhance vertical mixing and thus reduce the summer surface temperatures. Otherwise temperature error larger than 1 K only occur near coasts and could be caused by small scale features in the atmospheric circulation, which are not resolved by the atmospheric forcing applied to the ocean model, like e.g. the strong positive bias in winter in the Marmara Sea.

At the depth of the intermediate water masses (325 m) the simulated western Mediterranean temperatures are approximately 0.5 K warmer than climatology. In the eastern Mediterranean the pattern is characterized by slightly too cold water masses in the central Ionian and Levantine Seas, whereas coastal water masses are generally too warm (see Fig. 2). The simulated deep water masses (at 1401 m) are generally too warm: 0.8 K in the western Mediterranean, 0.4 K in the eastern basin (see Fig. 2).

The simulated surface salinity as well as the deviations from the MEDATLAS climatology are displayed in Figs. 3 and 4. Whereas the calculation of surface heat fluxes using bulk formulas with modeled SSTs as ocean input implies a damping feedback on the modeled SSTs towards the imposed original climatology, there does not exist a similar feedback for surface salinity. Thus salinity tends to accumulate all errors in the hydrological forcing and in the circulation. The general structure of the simulated surface salinity is quite realistic. The model simulates the structure of relative fresh water entering the Mediterranean along the Algerian coast and saltier water masses in

CPD
6, 2005–2054, 2010
Modeling Mediterranean ocean climate of the LGM
U. Mikolajewicz

the Balearic Sea. The structure in the eastern Mediterranean is characterized by the inflow of low salinity water from the west and recirculation of saltier water at the coasts. The outflow from the Bosphorus is spreading along the coast of Greece. The Adriatic is characterized by inflow of salty surface and subsurface waters from the Ionian in the east. In the west, the plume of the Po is spreading southward along the Italian coast.

The model somewhat overestimates the salinity in the northern and southern Ionian and underestimates the salinity in the Levantine. The overestimation of the Nile runoff is responsible for the strong negative anomalies along the eastern margin of the Levantine. Part of this signal, however, is likely to be an artifact due to insufficient representation of the plume of the Nile in the MEDATLAS climatology, both due to the reduction in Nile discharge as a consequence of the Aswan dam and due to too much spatial smoothing in the data processing. Whereas the northernmost part of the Adriatic is more than 1‰ too fresh, the central and southern parts are too salty, indicating an overestimation of the inflow of salty water from the Ionian. The model overestimates the low-salinity signal of the outflow from the Bosphorus in the northern and western Aegean.

At depth the model errors are much smaller than at the surface (see Fig. 4). A typical error at 325 m depth is −0.07‰ in the eastern basin and 0.05‰ in the western basin. At 1401 m depth, the errors are approximately 0.12‰ in the western basin and 0.03‰ in the eastern basin. It should be stressed that the water mass properties discussed here are entirely model generated and not spurious remainders of the initial conditions.

Sites of convective deep and intermediate water formation are indicated in Fig. 3. The climatological mixed layer depth maximum based on a potential density criterion of 0.05 $\mathrm{kg\,m^{-3}}$ relative to the surface density is used as proxy. In the western basin, the deep water is formed mainly in the Gulf of Lion. Some convection also takes place in the Ligurian Sea. In the eastern basin, deep water is formed in the Adriatic, and in the northwestern part of the Ionian. This pattern of deep winter mixed layer depths is largely consistent with the mixed layer climatology of D'Ortenzio et al. (2005). The mean mixed layer depth is a time average over potentially very different years. In some of the years the deep convection in the southern Adriatic actually reaches the model bottom, but as it does not in other years. The interpretation of deep or intermediate water formation has throughout this paper always been crosschecked with radioactive age tracers, which were included in these simulations.

By far the highest densities in the bottom layer are simulated in the northern Adriatic. Here the water flows southward along the western margin, filling the deep southern Adriatic. Together with water formed by open ocean convection in the southern Adriatic, this forms the deep overflow water entering the Ionian through the Strait of Otranto. The entrainment of less dense ambient water on the way to the south is quite large, which is a typical feature of insufficient resolution of plume flow in z-coordinate models. As a consequence of this entrainment the convection in the northwestern Ionian is overestimated.

Levantine intermediate water (LIW) is formed around Crete and between Crete and Cyprus, where the high salinities allow sufficient high densities. The pattern is - with the exception of the overestimation of the convection in the northwestern Ionian - quite realistic (Pickard and Emery, 1990).

In winter the Black Sea SST is approximately 1.5 K too warm, in summer the temperature error is smaller (approx. 0.5 K). The water at depth is too cold, 0.8 K at 325 m and 1.2 K at 1401 m. Whereas the surface water in the interior is slightly too salty, the deep water is much too fresh. However, the model drift in the Black Sea towards saltier conditions is still substantial, which certainly could be one explanation for the overestimation of convection in the central Black Sea, as this artificially destabilizes the water column. Nevertheless, the strong overestimation of the width of the Bosphorus in the model is a limiting factor for the ability of the model to realistically simulate the climate of the Black Sea.

The model simulates a deep outflow of 0.81 Sv through the Strait of Gibraltar. The inflow of Atlantic water is with 0.86 Sv slightly higher due to the need to compensate for the negative net freshwater flux. Bryden et al. (1994) estimated the time-average outflow of Mediterranean water through the Strait of Gibraltar from hydrographic measurements to be 0.68 Sv. Baschek et al. (2001) from current meter moorings 0.81 Sv. Older estimates where somewhat higher, Lacombe and Richez (1982) estimated this to be 1.15 Sv, Bethoux (1979) even 1.6 Sv. Thus the model outflow is quite realistic and consistent with actual estimates.

The near-surface circulation in run CTL shows in the western basin a strong Atlantic inflow in the southern part exiting through the Strait of Sicily into the eastern basin. The Gulf of Lion is characterized by a strong cyclonic circulation associated with the deep water formation cell (see Fig. 5). In the Tyrrhenian Sea the water flows first eastward north of Sicily and then follows the Italian coast northward. In the eastern basin, the continuation of the Atlantic inflow propagates as a mid-ocean jet into the Levantine basin. Together with a strong westward current along the Turkish coast, this forms the Rhodes gyre associated with the formation of Levantine intermediate water. Jointly with outflow water from the Black Sea, this feeds the northward surface flow along the Greek and Albanian coasts. The Adriatic shows a clear cyclonic circulation, which is mostly a summer and fall phenomenon. The surface circulation in the Black Sea is cyclonic as well. The general circulation pattern agrees quite well with the findings presented by Pinardi and Massetti (2000).

The hydrological cycle of the model (see Table 1) is a combination of prescribed quantities (precipitation and river runoff), which were derived from the ECHAM5 T106 simulations, and interactively calculated evaporation, which depends on the model SST. In the control simulation, the Mediterranean gains 32 100 $m^3 s^{-1}$ from precipitation, 11 300 $m^3 s^{-1}$ from river runoff and loses 97 300 $m^3 s^{-1}$ by evaporation. The Black Sea and the Marmara Sea have a net surplus of freshwater of 6900 $m^3 s^{-1}$, which is dominated by river input. Thus the net freshwater loss east of the Strait of Gibraltar is 47 100 $m^3 s^{-1}$, which corresponds to the net inflow from the Atlantic.

The basin mean (Mediterranean only) of the prescribed precipitation is 0.4 m/yr. This agrees quite well with the results from NCEP and ECMWF reanalyses (0.43 and 0.33 m/yr for the years 1979 to 1993 according to Mariotti et al., 2002). The classical estimates from observation are somewhat higher than these value: 0.55 (Jaeger,

CPD
6, 2005–2054, 2010

1976), 0.7 m/yr (Legates and Willmott, 1990) and 0.48 m/yr (CMAP, Xie and Arkin, 1998). The basin mean calculated evaporation is 1.17 m/yr. The mean values (1979–1993) from the reanalysis of NCEP and ECMWF are 0.93 and 1.11 m/yr. Estimates from observations are slightly higher with 1.21 (Jaeger, 1976), 1.36–1.54 (Bethoux and Genitili, 1999) and 1.18 m/yr (Mariotti et al., 2002). Both precipitation and evaporation are close to estimates from observations and reanalysis data.

The total freshwater budget of the Black Sea is quite realistic and close to observations (e.g. Tolmazin, 1985). The range of river discharge rates for the Mediterranean given in the review paper by Ludwig et al. (2009) lies with 12 700 to 14 300 $m^3 s^{-1}$ close to the model value of 11 300 $m^3 s^{-1}$. The corresponding value for the Black Sea are 11 100 to 12 700 $m^3 s^{-1}$ compared to 11 700 $m^3 s^{-1}$ from the model.

Bryden et al. (1994) estimate the total freshwater loss of the Mediterranean from hydrographic measurements in the Strait of Gibraltar to be 0.52 m/yr. The total freshwater loss of the model east of Gibraltar is 47 100 $m^3 s^{-1}$ corresponding to 0.57 m/yr if related to the area of the Mediterranean. Earlier estimates from hydrographic data yield – consistent with the higher outflow rates and similar salinity differences between inflowing and outflowing water at Gibraltar – higher estimates of the net evaporation of the Mediterranean Sea: e.g. 0.75 m/yr (Lacombe and Richez, 1982) and 0.95 m/yr (Bethoux, 1979). Estimates involving precipitation and evaporation from reanalyses tend to be somewhat lower (between 0.37 and 0.52 m/yr, see e.g. Mariotti et al., 2002). In general, the hydrological cycle of this model is well within the estimates from both observations and from reanalysis data.

4 Boundary conditions LGM

For the LGM simulation, the topography was modified adding the anomalies from the ICE-5G reconstructions (Peltier, 2004) between 21 and 0 kyrBP to the standard topography. This resulted in reductions of the water depth between 127 m in the interior of the basin and 98 m in coastal areas (see Fig. 1 bottom). The Bosphorus is closed and thus the Black Sea no longer part of the model. The sill depth at the Strait of Gibraltar has been reduced from 256 to 156 m.

The near-surface air temperatures are much colder than in the control simulation (see Fig. 6). In February, the temperature anomaly is characterized by a strong north-south gradient with a cooling exceeding 10 K over the Alps and on the Balkan and a cooling of less than 3 K in the northeastern Sahara and on the Arabian peninsula. The cooling is particularly strong in that part of the northern Adriatic which is converted to land due to the lower sea level. The changes in albedo and the strongly reduced heat capacity are responsible for this strong winter cooling signal.

In August, the simulated near-surface air temperature anomaly shows a clear east-west gradient. In central Spain, the simulated summer cooling reaches 9 K, in the northern half of Italy, it exceeds 7 K, whereas the cooling in the land areas around the eastern Levantine is typically 5 K. Over the Mediterranean, the simulated cooling of air temperature anomalies is reduced compared to the land signal, but the longitudinal gradient is similar.

Temperatures over the Mediterranean land areas have been reconstructed from pollen data. Wu et al. (2007, their Fig. 8) estimated the temperature of the coldest month at LGM to be between 6 and 19 K colder than present, the temperature of the warmest month between 2 and 11 K.

The anomalies of precipitation minus evaporation (from the atmospheric model) over the Mediterranean are in general positive (see Fig. 6). The strongest local changes occur in those regions which are converted from ocean to land. The changes in precipitation are positive for the eastern Mediterranean and the Tyrrhenian Sea, whereas they are rather small in the western basin (cw. Fig. 6). The enhanced precipitation in the eastern Levantine is consistent with higher sea levels of the Dead Sea (Stein et al., 2009). Integrated over the basin, precipitation is slightly reduced, which reflects mostly the effect of the reduced area (see Table 1). Over the Mediterranean, evaporation is reduced due to the lower temperatures. Thus the positive signal in precipitation minus evaporation is much larger than the precipitation signal. The simulated precipitation is

CPD
6, 2005–2054, 2010

enhanced over the source regions of the Nile. The consequence is a strongly enhanced discharge from the Nile. It almost doubles compared to the control state. Reeder et al. (2002) estimated from the lack of turbidites that Nile discharge is strongly reduced during the LGM. Almogi-Labin et al. (2009) report a considerable Nile discharge during the LGM from sediment cores in the Levantine. The runoff from Spain, France, the Alps, Italy and Croatia is strongly enhanced as well due to enhanced precipitation. As a consequence, the total river runoff into the Mediterrenian is increased by 70% compared to present day (see Table 1). The integrated evaporation (calculated in the ocean model) is reduced by 20%. The reduced evaporation is the major contribution to the reduced freshwater loss of the Mediterranean (28,200 compared to 47 100 $m^3 s^{-1}$ for CTL). The enhanced river runoff compensates for the missing outflow from the Black Sea.

The simulated precipitation changes in tropical eastern Africa vary considerably between the different models. The high resolution atmosphere-only simulation from Kim et al. (2008) seems to show higher precipitation. On the other side, Braconnot et al. (2007) report reduced precipitation as the mean outcome from several coupled atmosphere-ocean GCMs. Results from several high resolution simulations for Europe with different models did not show a consistent picture for the changes in precipitation in the Mediterranean region (Jost et al., 2005, their Fig. 5).

Wu et al. (2007) estimated reduced precipitation around the Mediterranean and in tropical east Africa from pollen data using an inverse vegetation model. Farrera et al. (1999) estimated from various proxy data reduced precipitation in tropical east Africa, but increased precipitation minus evaporation. Lake levels around the Mediterranean were higher, although only few data are available (Kohfeld and Harrison, 2000). In tropical east Africa, lake level data are inconclusive, about as many data hint to wetter conditions as to dryer conditions.

5 Results LGM

The baseline LGM simulation has been integrated for 1699 years. The remaining drift in the Mediterranean over the last 300 years is 0.004 K/century for the basin mean temperature at 2029 m depth. For salinity, the drift is 0.003‰/century at the surface and 0.004‰/century at 2029 m depth.

5.1 Temperature

The simulated SSTs are shown in Fig. 7 together with reconstructions derived from marine sediment cores. Temperatures have been estimated from assemblages of planktonic formanifera with two different methods (Hayes et al., 2005): The revised analog method (RAM, Waelbroeck et al., 1998) and the artificial neural network technique (ANN, Malmgren et al., 2001). For annual mean temperatures, additional estimates derived from alkenones have been used (Lee, 2004, and references therein).

Both model and reconstructions agree on the general SST pattern for winter. The coldest temperatures occur in the Gulf of Lion and the Adriatic. The RAM estimates are somewhat warmer than the ANN estimates. In general, the model agrees reasonably well with both reconstructions. The model is too warm in the Alboran Sea, which can be explained by the combined effect of the lack of tidal mixing in the Strait of Gibraltar and the forcing. The ESM simulation showed only a moderate cooling in the Gulf of Cadiz in contrast to reconstructions. Thus the cooling between LGM and present of the inflowing Atlantic water is underestimated, which results in an overestimation of the surface temperatures in the Alboran Sea.

The temperature pattern in summer is quite similar. SSTs are cold in the north and warm in the southeastern Levantine. In the eastern basin, the agreement between model and the ANN reconstruction is reasonable. The estimate based on the RAM method is somewhat colder than the ANN reconstruction. In the Adriatic and east of Greece, the simulated SSTs are several degrees too warm compared to the proxy estimates. In the entire western Mediterranean the simulated SSTs are substantially warmer than the proxy estimates. At this time of the year, however, there exists a strong vertical temperature gradient, with typical temperature differences between the surface and 37 m of 2 to 5 K (see Fig. 8). At this depth, the deviation between reconstructed and simulated temperatures in the western Mediterranean is much smaller than at the surface.

For the annual mean, the model reproduces the reconstructions in the eastern Mediterranean quite well, but is too warm in the western Mediterranean and the Alboran Sea due to the mismatch in summer. The annual mean temperatures have been reconstructed from alkenones (Lee, 2004, and references therein) as well. Whereas in the western Mediterranean these estimates agree quite well with the estimates from assemblages of foraminifera, the alkenone derived temperatures in the eastern Mediterranean are substantially colder than the other estimates. In this region, two of the three estimates from the core top in the data set supplied by Lee (2004) deviate by more than 4 K from present annual mean climatology. Emeis et al. (2000) have suggested that alkenones in Mediterranean record winter and spring temperatures rather than annual mean temperatures. The alkenone temperatures in the eastern Mediterranean are as cold or even colder than the closest estimates for winter temperatures from Hayes et al. (2005), cw. Fig. 7).

The anomalies between LGM and CTL are shown in Fig. 9. As for the reconstructions from assemblages of foraminifera no equivalent estimates of present surface temperatures are available, the data have been compared to observed hydrographic climatology. Following Hayes et al. (2005) the WOA (1998, henceforth WOA98) climatology is used. A comparison with temperature estimates derived with the same method from core top assemblages of foraminifera would clearly have been preferable, but these data are not available. Thus, this inconsistency introduces an additional source of error for the reconstructed temperature anomalies.

The simulated cooling in winter (Fig. 9) shows values around 2.5 K in the Levantine and 4.5 K in the northwestern Mediterranean. The Adriatic shows the strongest cool-

CPD
6, 2005–2054, 2010

ing with values up to 8 K. The anomalies of reconstructed winter temperatures relative to observed instrumental data show a quite similar pattern with a weak cooling in the Levantine and maximal cooling (more than 6 K) of the northwestern Mediterranean. The model underestimates the cooling in the inflowing Atlantic water, which is a consequence of the forcing from the global ESM. In the reconstructions, the winter cooling in the Adriatic is rather small, clearly not consistent with the strong cooling in the model. However, the two reconstruction methods show large deviations at this location. The ANN proxy estimates yield systematically smaller climate changes than the RAM estimates. Temperature differences between the two estimates of 2 K are not infrequent.

The simulated change in summer SST (Fig. 9) is dominated by the strong east-west gradient with a weak cooling (2 to 3 K) in the Levantine and more than 6 K in the Gulf of Lion and the Adriatic. The general pattern of temperature change derived from the proxy estimates is quite similar, but the model underestimates especially the cooling in the western Mediterranean, which amounts to values of 10 K or more in the proxy reconstructions. There is, however, a substantial depth dependence of the simulated temperature anomaly, as is revealed in a comparison of the summer surface temperature signal with the signal at 37 m depth.

The simulated annual mean SST difference between LGM and CTL (Fig. 9) shows the same gradient between the Levantine and the Gulf of Lion as the summer and winter signals. With respect to reconstructions, the model underestimates this gradient. In general, the model is closer to the ANN reconstructions. The alkenone derived temperature changes (relative to the core top data) suggest slightly less cooling in the western Mediterranean than the Hayes et al. (2005) estimates. In the eastern Mediterranean the cooling derived from alkenones ranges from 2.7 to 10.1 K. This suggests that these data might not only record changes in annual mean temperature, but potentially also changes in season and/or depth of the plankton production.

The reconstructions from assemblages of foraminifera have formally been performed for temperatures at 10 m depth, but the foraminifera are living over a wider depth range. Thus, it might be more appropriate to compare the estimates with the temperatures

CPD
6, 2005–2054, 2010

integrated over a depth range corresponding to the habitat of the foraminifera. Doing this in a proper way would require to repeat the estimation of the transfer function using depth integrated temperatures as input data. In winter this problem is not relevant as the vertical temperature gradient is small due to the deeper winter mixed layers.

An earlier estimate of LGM SSTs in the Mediterranean by Thiede (1978) agrees quite well with the general pattern of the simulated SST differences between LGM and present. Thiede (1978) reports the presence of a rather cold water mass protruding in a narrow tongue southward from the eastern Aegean as far south as 33° N, which is absent in the reconstruction from Hayes et al. (2005) and in the simulations. Bigg (1994) reported a change in simulated annual mean SST between their LGM and control simulations with a clear east west gradient with more than 4 K cooling in the Alboran Sea and less than 1 K at the Libyan coast.

In the simulation of the LGM in the atmosphere model, the orographic forcing exerted by the Fennoscandian ice sheet causes a southward displacement of the belt of westerly wind in the troposphere over Europe. This leads to the advection of colder moist air into the northwestern Mediterranean. This results in enhanced cloud cover and precipitation over Spain, southern France and northern Italy. The increased soil moisture amplifies the evaporative heat loss and thus the surface cooling. The shortwave radiation reaching the surface is reduced here and over the western Mediterranean due to the enhanced cloud cover with a maximal effect in the Gulf of Lion (approximately $12\,\mathrm{W/m^2}$ less absorbed shortwave radiation than in CTL). The northerly near-surface winds over the northwestern Mediterranean amplify the advection of cold air onto the Gulf of Lion, leading to a cooling of the ocean surface by sensible heat flux. The stronger winds enhance vertical mixing, thus distributing the summer warming over a wider depth range in run LGM than in CTL (see Fig. 8). The wind induced mixing is increased in JJA by almost 50% in the northwestern Mediterranean, in the Tyrrhenian Sea by even 67%. The result is a rather strong surface cooling in run LGM in the northwestern Mediterranean compared to the rest of the Mediterranean. At 37 m depth this anomalous cooling pattern has essentially vanished, creating a cooling pattern which

CPD
6, 2005–2054, 2010

is very similar to the winter pattern. The ability of the model to reproduce this pattern realistically in CTL becomes obvious by comparison with the MEDATLAS climatology.

At 1401 m depth the simulated cooling between LGM and CTL is approximately 3.1 K in the Ionian and the Levantine and 4.7 K in the western basin.

The basin averaged annual long-term mean heat loss from the Mediterranean (see Table 2) is almost unchanged. The reduced heat loss by evaporation is compensated by increased heat loss by sensible heat fluxes and longwave radiation. The reduction in downward longwave radiation is only partially compensated by the reduced upward longwave radiation.

5.2 Circulation and salinity

During the LGM the global mean salinity was approximately 1‰ higher than today due to the lower global sea level. The salinity anomaly for the Atlantic, which was derived from simulations with the coarse resolution ESM, is close to this value. The simulated surface salinity anomaly in the Mediterranean is substantially higher than this (see Fig. 10). The western Mediterranean is saltier by approximately 1.9‰ with higher values in the Tyrrhenian, the eastern Mediterranean by slightly less than 2‰ and in Levantine compared to CTL. East of Sicily, in the region with deep convection in LGM, the salinity anomaly is almost 3‰. The salinity here has typical values between 40.8 and 40.9‰ only, about 0.1‰ lower than the salinity maximum in the central Levantine. Regions with reduced salinities are the Adriatic and the plume of the Nile, which is extended in the LGM simulation due to the enhanced discharge from the Nile. In the Aegean, the increase of the salinity reaches maximal values, which is a consequence of the lacking outflow from the Black Sea and the associated tongue of relative fresh water in the northern and western Aegean (cw. Fig. 10). At a depth of 1401 m the salinity increase is 2.1‰ in the eastern basin 1.7‰ in the western basin (not shown).

Using strongly simplifying assumptions, Thunell and Williams (1989) estimated that the eastern Mediterranean was saltier by 2.7‰ compared to today, which is in good agreement with the model result. Their estimate of the salinity changes in the western

CPD
6, 2005–2054, 2010

Mediterranean is 1.2‰. Myers et al. (1998) estimated even higher values for the salinity increase in the Levantine and used them as forcing for their model simulations.

Bigg (1994) showed only small changes in salinity between his LGM and CTL simulations, but his simulation was much too short (21 years) for substantial salinity anomalies to develop and it is rather unlikely that a steady state was reached. The control simulation of Bigg (1994) revealed massive problems to reproduce the current Mediterranean ocean climate (e.g. an outflow from the Strait of Gibraltar of 0.1 Sv, no deep water formation neither in the eastern nor in the western Mediterranean) and his simulations were much too short. His simulated change in annual mean SST showed a clear east west gradient with more than 4 K cooling in the Alboran Sea and less than 1 K at the Libyan coast.

In the LGM simulation, the spatially reduced Adriatic has turned into an estuarine basin due to the higher river runoff without deep convection (see Fig. 10). Deep water formation in the eastern basin is concentrated in the northern Ionian. The highest surface salinities (except for some almost isolated coastal points) are simulated in the central and southwestern Levantine. However, densities are not high enough to allow the formation of Levantine intermediate water, which can be attributed both to the reduced difference in salinity in the region of deep convection and to the relatively low winter cooling. The increased Nile discharge reduces the increase in surface salinities in the Levantine.

In the western Mediterranean, the Gulf of Lion is the main source of deep water in LGM. Here the local surface salinity reaches a maximum due to the mixing of surface waters with underlying warm and salty outflow water originating from the Strait of Sicily. By exposing this salty water to strong surface cooling, sufficiently dense water is formed. A similar process takes place in the western Tyrrhenian Sea resulting in formation of deep intermediate and occasionally even deep water.

Various attempts have been made to test for the potential existence of multiple steady states of the Mediterranean circulation. All simulations seem to converge towards a similar state. The formulation of the boundary conditions with calculation of the heat fluxes from bulk formulas using atmospheric quantities and the actual model SST is a variant of the so called mixed boundary conditions (restoring of the SST towards a prescribed value and flux condition without restoring for salinity), which for the global ocean are known to overestimate the sensitivity of deep water formation cells towards perturbations (e.g. Mikolajewicz and Maier-Reimer, 1994). In the Mediterranean, however, this problem is probably less severe, as there are no strong oceanic heat transports involved, which could be modified and feed back onto the atmosphere. Additionally the Mediterranean is much smaller and surrounded by land, which also should make the formulation of the thermohaline boundary condition more appropriate for the current problem than for the problem of investigating the stability of the thermohaline circulation of the global ocean.

Myers et al. (1998) obtained quite different changes in deep water formation. In their LGM simulation, the main site of deep water formation in the eastern basin was the Rhodes gyre region. For the LGM they prescribed the strongest salinity increase at the eastern margin of the Levantine. The anomaly pattern prescribed in their simulations is quite different from the pattern obtained in the simulations presented here, where the strongest increase in surface salinity occurs east of Sicily and in the Aegean (see Fig. 10). Thus, the completely different response of the circulation can be explained by their prescribed surface salinity anomaly. Their simulation shows an estuarine circulation in the Adriatic as well.

The deep outflow of Mediterranean water through the Strait of Gibraltar reaches only 0.40 Sv, approximately 50% of the 0.81 Sv in CTL. The corresponding inflow is given by the necessity to balance the outflow and the net freshwater loss of the Mediterranean. The density difference between Mediterranean water and the ambient Atlantic water increases from 2 $\mathrm{kg\,m^{-3}}$ to 3 $\mathrm{kg\,m^{-3}}$. In both cases the gradient has been estimated on the model level above the sill. The salinity difference increases from 2.5 to 3‰. In LGM the outflowing Mediterranean water is approx. 2 K colder than the water in the Gulf of Cadiz. This increases the density difference, whereas in CTL the temperature difference between Alboran Sea and Gulf of Cadiz is small and the density difference is almost entirely determined by salinity. The deep outflow from the Ionian Sea through the Strait of Sicily is reduced from 1.06 Sv to 0.65 Sv.

A similar reduction of the outflow of Mediterranean water through the Strait of Gibraltar has been found in the model study of Myers et al. (1998) with a somewhat stronger outflow. Bigg (1994) did not simulate substantial changes in Mediterranean outflow through the Strait of Gibraltar.

The reduction in transport through the Strait of Gibraltar by a factor of 2 is consistent with the reduction that would be caused by the lower sea level and the reduced cross-sectional area of the strait under the assumptions of hydraulic control in the Strait and overmixing in the Mediterranean (Bryden and Stommel, 1984; Rohling and Bryden, 1994).

Using the analytical model of hydraulic control, Rohling and Bryden (1994) yield of reduction of the outflow to 53% of the present value due to a change in sill depth corresponding to the one applied in our simulations. In a sensitivity experiment with present-day forcing but with the sill depths in the Straits of Sicily and Gibraltar reduced to LGM values, the Gibraltar outflow was reduced to 53% of CTL, which is identical to the results from the simple model. Taking into account the changes in net evaporation of the Mediterranean E_M to 60% of the CTL value E_{M0} would lead to a further decrease. Rohling and Bryden (1994) suggested a dependence of the outflow of Mediterranean water Q_M on the net evaporation E_M relative to a reference state (indicated by the additional subscript 0, the subcript M indicates Mediterranean properties)

$$\frac{Q_M}{Q_{M0}} = \sqrt[2]{\frac{E_M}{E_{M0}}}. \tag{1}$$

This would yield an additional reduction to 41% of the CTL value, thus overestimating the effect compared to the numerical model. Rohling (1999) used the dependence

$$\frac{Q_M}{Q_{M0}} = \sqrt[3]{\frac{E_M}{E_{M0}}} \tag{2}$$

based on results from the box model described by Matthiesen and Haines (2003). This relation yields a total reduction to 45% of the CTL value. Both formulas overestimate the reduction in outflow (to 41 and 45%, respectively compared to 50% of the numerical model) as they do not take the temperature contribution to the density gradient into account, which enhances the outflow and thus compensates largely for the effect of the reduced net evaporation.

Following e.g. Bryden and Kinder (1991), the Mediterranean outflow through the strait of Gibraltar Q_M can for the case of hydraulic control and overmixing be expressed as

$$Q_M = \alpha \sqrt{\frac{\Delta\rho}{\rho_M} g w^2 h^3} \tag{3}$$

where ρ is the potential density, w and h are width and depth of the Strait of Gibraltar. α is a dimensionless factor. Bryden and Stommel (1984) estimate it to be 0.25 with the assumption that the interface between the two layers is at half depth. Farmer and Armi (1986) showed that the lower layer has to be thinner and give $\alpha = 0.208$ for the maximum exchange solution.

If the density difference between lower and upper layer in the Strait of Gibraltar $\Delta\rho$ is entirely determined by the salinity difference, it can be expressed as $\beta\Delta S$, where β is the derivative of the density with respect to salinity. For a steady state, the equations of salt and mass conservation yield

$$\Delta S = \frac{E_M}{Q_M} S_A, \tag{4}$$

where the subscript A indicates Atlantic properties.

Combining Eqs. (3) and (4) yields

$$Q_M = \sqrt[3]{\alpha^2 \frac{\beta S_A}{\rho_M} h^3 w^2 g E_M}. \tag{5}$$

CPD
6, 2005–2054, 2010

Neglecting the changes in ρ_M leads immediately to the conclusion that the Mediterranean outflow Q_M is proportional to the depth of the strait and the third root of the net freshwater loss of the Mediterranean E_M. The long-term mean exchange through the Strait of Gibraltar in the model is clearly subcritical, but the flow in the strait is quite variable due to the variable forcing.

At first the increased salinity gradient between the Mediterranean and the Atlantic for the LGM seems to be counterintuitive in view of the fact that the net freshwater loss for the LGM is only 60% of the present value. However, the effect of the reduced exchange across the straits due to the lower sill depths, which leads to longer exposure times of the Mediterranean water masses to a net evaporation, is dominating (see below in the next subsection).

The changes in the meridionally integrated zonal stream function (see Fig. 11) show the formation of eastern Mediterranean deep water around 15° E and its subsequent eastward spreading. The formation of deep water in the Gulf of Lion around 5° E is not captured well by this quantity, as much of the spreading occurs southward. Only the deep inflow into the Tyrrhenian Sea around 10° E as a negative cell and the deep outflow into the Alboran Sea are captured by this quantity. In LGM, the main overturning cell with intermediate water becomes shallower due to the shallower sills and the intensity is reduced in accordance to the overflows over the sills. In both simulations, salty surface waters are downwelled to the depth of intermediate water in the southern part of the Levantine, while upwelling is predominant in the northern part.

In LGM, the near-surface currents especially in the western basin intensify (see Fig. 12) due to enhanced wind forcing. Apart from a strong cyclonic gyre in the Tyrrhenian, the basic current structure is similar. The changes in the eastern basin are substantial. The cyclonic circulation in the Adriatic has vanished. The closure of the Bosphorus leads to strong changes in the surface circulation of the Aegean. The northern Ionian is characterized by a strong cyclonic gyre. The eastward flow along the coast Egypt has substantially weakened.

CPD
6, 2005–2054, 2010

5.3 Sensitivity experiments

One of the main uncertainties in the LGM experiment is the hydrological forcing, especially the Nile discharge. In order to test the potential effect of inadequate hydrological forcing, two sensitivity experiments for the LGM were carried out. In experiment LGM-N2 the discharge of the Nile was doubled compared to LGM, in experiment LGM-N0 the Nile was completely eliminated. The annual mean changes in net freshwater flux of the Mediterranean resulting from this relative to LGM are ±9700 $m^3 s^{-1}$. Both simulations were started in year 99 from the same state as LGM and integrated for 1100 additional years. At the end of the simulations, they still show a small drift towards higher salinity, but the general circulation pattern has stabilized. Surface salinity and convection depths from these experiments are shown in Fig. 13. As salinity is still slightly increasing, convection might be slightly overestimated compared to the expected final state, which can be derived from the standard LGM simulation (not shown).

It is obvious from comparison of Figs. 10 and 13 that the Nile discharge has a strong influence on the surface salinities in the eastern Mediterranean. A removal of the Nile increases the surface salinities in the eastern Mediterranean by approx. 0.7‰, a doubling reduces them by 0.9‰. In the western basin the effects on a basin average are approximatel 50% of the effects in the estern basin, but the southern part is affected only weakly, as it is dominated by the properties of the inflowing Atlantic water. For both basins the salinity at depth strongly follows the changes in the eastern basin. The plume of the Nile discharge propagates in a cyclonic circulation near the coast around the Levantine. The consequence of a reduction of the Nile discharge is a reversed east-west salinity gradient in the eastern Mediterranean. The smaller the Nile discharge, the higher is the salinity gradient between the Rhodes gyre and the northern Ionian. With a doubled Nile discharge the gradient is reversed and the highest salinities are found in the Ionian. These changes in the salinity gradient have immediate consequences for the amount of LIW formed: Whereas it is absent in simulation LGM-N2 it is strongly enhanced in simulation LGM-N0. In the latter simulation, a substantial amount of dense water is formed in the Aegean, but it is, when reaching the Levantine, not dense enough

CPD
6, 2005–2054, 2010

to form bottom water, it only penetrates to 1200 m depth. This, however, could be an artifact due to the model's difficulties to represent deep overflow plumes adequately. In run LGM-N0, the centers of convection in the Ionian is shifted towards northeast. Deep convection occurs at the continental slope off western Greece. In run LGM-N0 the convection in the Tyrrhenian is strongly reduced due to the higher density of the water passing through the Strait of Sicily.

The anomalies in sea surface temperatures between these three LGM simulation (not shown) are generally small due to the formulation of the upper boundary condition for temperature. In experiment LGM-N0 the deep temperatures in the eastern basin are generally somewhat warmer due to the higher contribution of LIW. This effect is as large as 0.4 K on a basin average around 400 m. In the western basin the entire deep part is warmer by 0.6 to 0.8 K.

The circulation changes in experiment LGM-N0 with suppressed Nile discharge are much more similar to the circulation changes found in Myers et al. (1998) than the baseline LGM simulation, however, deep water formation in the northern Ionian is important in all LGM simulations.

The outflow rates of Mediterranean water through the Strait of Gibraltar in the experiments LGM-N0, LGM and LGM-N2 are 0.44, 0.40 and 0.34 Sv. The relation between deep westward flow through the Strait of Sicily and the net evaporation in the eastern Mediterranean is similar. The outflow rates in the three experiments are 0.70, 0.63 and 0.48 Sv with a net freshwater loss of the eastern Mediterranean in run LGM of 19 000 $m^3 s^{-1}$. For both straits the model results suggest for the LGM $Q_i \propto E_i^{1/3}$, where Q is the outflow through the strait and E the net freshwater loss east of the respective strait.

In the sensitivity experiment SILL the effect of the lower sills in the LGM is investigated. The only difference in the set up to run CTL are modifications of the sill depths of the Straits of Gibraltar and Sicily to LGM values. This run was initialized from year 499 of CTL and integrated for 600 years. The lowered sill depth of the Strait of Gibraltar resulted in a reduction of the Mediterranean outflow to 0.43 Sv. The hydrological

CPD
6, 2005–2054, 2010

budget was almost unchanged. Due to the longer residence times, the salinity inside the Mediterranean increased (see Fig. 10bottom). In the eastern basin the mean surface salinity increased by 1.8‰. The formation of LIW is increased compared to run CTL. In the western basin the reduced amount of inflowing Atlantic water penetrates further to the north than in CTL. The outflow through the Strait of Sicily of 0.94 Sv is – in spite of the reduced sill depth – even slightly higher than in the control simulation (0.91 Sv.

Variations in the flow through the Strait of Gibraltar due to changes in evaporation and sill depth between the different experiments show a similar relation, as would be expected by hydraulic control and the assumption of overmixing (see Eq. 5), although the flow – at least in the long-term mean – is subcritical.

5.4 Effect of downscaling

The comparison of the SST anomalies simulated by the regional model (see Fig. 9) compared to the anomalies simulated by the coarse resolution ESM (see Fig. 14) shows quite some similarity, indicating that the response in SST is modified only to a small degree by the downscaling. The coarse resolution ESM (atmospheric resolution approx. 3.75°, ocean resolution in the Mediterranean between 180 and 250 km) simulates essentially the spatial gradients in SST change between LGM and CTL found also in the regional model. Due to the lack of resolution the changes in the exchange across the Straits of Gibraltar and Sicily are not reproduced well. Thus the ESM produces a larger gradient between Atlantic and Levantine salinity during the LGM. Reliable estimates of changes in deep water formation inside the Mediterranean etc. are beyond the capability of the ESM.

Attempts to force the regional ocean model directly with the atmospheric forcing from the ESM failed to produce a realistic ocean climate. Especially the wind stress forcing turned out to be a major problem preventing a realistic surface circulation inside the Mediterranean. The use of a coupled regional atmosphere-ocean model could further increase the effective resolution, but the required spin-up times of more than 1000 years are prohibitively expensive.

CPD
6, 2005–2054, 2010

6 Summary and conclusions

With a chain of model simulations it was possible to reproduce the pattern of Mediterranean surface temperature change between LGM and present, although the summer cooling in the Gulf of Lion is underestimated. This pattern is almost entirely set by the simulation with the coarse resolution ESM. This can be explained by the temperature restoring, which is implicit in the use of calculating heat fluxes from bulk formulas with prescribed atmospheric input data and modeled SST. Only in regions with strong changes in air-sea heat exchange (like e.g. regions with deep convection or intense upwelling) substantial changes in SST can occur.

The strong summer cooling in the northwestern Mediterranean in LGM relative to present can be explained by moister conditions in the northwestern Mediterranean and the adjacent land areas resulting in enhanced humidity and reduced shortwave radiation reaching the surface and by changes in the vertical temperature structure of the ocean. Whereas in the CTL simulation the vertical near-surface ocean temperature gradient is quite large, the stronger winds and the associated enhanced vertical mixing substantially reduces this stratification distributing the reduced summer warming over a larger depth interval. The consequence is a strong surface cooling between LGM and present, but only a moderate cooling at the levels immediately below. This aspect has so far not been accounted for in the reconstructions. Here a consideration of the depth, where the plankton actually is living, might improve the realism of the reconstructions.

The presence of a small ice sheet or enhanced glaciation in the Alps in the ESM setup could have enhanced the cooling over land and thus amplified the episodic cooling by northerly winds. This would impose a strong cooling in the Gulf of Lion and a weak additional cooling in the western Mediterranean. This could reduce the difference in the amplitude between modeled and reconstructed summer SST in the northwestern Mediterranean.

Whereas the changes in deep water formation pattern are moderate in the western Mediterranean, the differences in eastern Mediterranean deep water formation are

CPD
6, 2005–2054, 2010

substantial. Deep convection in the LGM simulation is concentrated in the region east of Sicily, LIW formation in the Rhodes gyre is only weak. However, the changes in the eastern basin are strongly sensitive to the strength of the Nile discharge. In the LGM simulation the Adriatic is an estuarine basin, whereas it is the main source of deep water in CTL. The lowered sea level during LGM results in reduced sill depths for the Straits of Gibraltar and Sicily. The consequence is reduced exchange across the sills which in turn leads to stronger salinity enrichment in the Mediterranean in relation to the inflowing Atlantic water than at present in spite of reduced net evaporation during LGM.

Acknowledgements. This work was in part performed within the project HOBIMED, funded by the Deutsche Forschungsgemeinschaft within the cooperative project INTERDYNAMIK. The computations have been performed at the DKRZ. The motivation for this work arose from discussions with Michal Kucera. Discussions with Fanny Adloff, Rosina Grimm Alfredo Izquierdo, and Ernst Maier-Reimer helped to improve this manuscript substantially. The paper was written during a visit at SMHI.

The service charges for this open access publication
have been covered by the Max Planck Society.

References

Almogi-Labin, A., Bar-Matthews, M., Shriki, D., Kolosovsky, E., Paterne, M., Schilman, B., Ayalon, A., Aizenshtat, Z., and Matthews, A.: Climatic variability during the last 90 ka of the southern and northern Levantine Basin as evident from marine records and speleothems, Quaternary Sci. Rev., 28, 2882–2896, 2009. 2007, 2018

Arpe, K., Leroy, S. A. G., and Mikolajewicz, U.: The last glacial maximum locations of summer-green tree refugia using simulations with ECHAM3 T42 uncoupled, ECHAM5 T31 coupled and ECHAM5 T106 uncoupled models, Clim. Past Discuss., 6, 537–584, doi:10.5194/cpd-6-537-2010, 2010. 2009

Baschek, B., Send, U., Lafuente, J. G., and Candela, J.: Intensive shipboard observations of the flow through the Strait of Gibraltar, J. Geophys. Res., 106 (C12), 31017-31032, 2001. 2015

Bethoux, J. P.: Budgets of the Mediterranean Sea: Their dependence on the local climate and on the characteristics of the Atlantic waters, Oceanol. Acta, 2, 157–163, 1979. 2015, 2016

Bethoux, J. P. and Gentili, B.: Functioning of the Mediterranean Sea: Past and present changes related to freshwater input and climatic changes, J. Mar. Syst., 20, 33-47, 1999. 2016

Bigg, G .R.: An ocean general circulation model view of the glacial Mediterranean thermohaline circulation, Paleoceanography, 9, 705–722, 1994. 2007, 2008, 2011, 2022, 2024, 2026

Braconnot, P., Otto-Bliesner, B., Harrison, S., Joussaume, S., Peterchmitt, J.-Y., Abe-Ouchi, A., Crucifix, M., Driesschaert, E., Fichefet, Th., Hewitt, C. D., Kageyama, M., Kitoh, A., Lan, A., Loutre, M.-F., Marti, O., Merkel, U., Ramstein, G., Valdes, P., Weber, S. L., Yu, Y., and Zhao, Y.: Results of PMIP2 coupled simulations of the Mid-Holocene and Last Glacial Maximum Part 1: experiments and large-scale features, Clim. Past, 3, 261–277, doi:10.5194/cp-3-261-2007, 2007. 2009, 2018

Bryden, H. L., Candela, J., and Kinder, T. H.: Exchange through the Strait of Gibraltar, Prog. Oceanogr., 33, 201–248, 1994. 2014, 2016

Bryden, H. L. and Kinder, T. H.: Steady two-layer echange through the Strait of Gibraltar, Deep-Sea Res., 38, Suppl. 1, S445–S463, 1991. 2027

Bryden, H. L. and Stommel, H. M.: Limiting processes that determine basic features of the circulation in the Mediterranean Sea, Oceanol. Acta, 7(3), 289–296, 1984. 2007, 2026, 2027

D'Ortenzio, F., Iudicone, F., Montegut, C. D., Testor, P., Antoine, D., Marullo, S., Santoleri, R., and Madec, G.: Seasonal variability of the mixed layer depth in the Mediterranean Sea as derived from in situ profiles, Geophys. Res. Lett., 32, L12605, doi:10.1029/2005GL022463, 2005. 2013

Emeis, K.-C., Struck, U., Schulz, H.-M., Bernasconi, S., Sakamoto, T., and Martinez-Ruiz, F.: Temperature and salinity of Mediterranean Sea surface waters over the last 16,000 years: constraints on the physical environment of S1 sapropel formation based on stable oxygen isotopes and alkenone unsaturation ratios, Palaeogeography, Palaeoclimatology, Palaeoecology, 158, 259–280, 2000. 2020, 2047

Emeis, K.-C., Schulz, H., Struck, U., Rossignol-Strick, M., Erlenkeuser, H., Howell, M. W., Kroon, D., Mackensen, A., Ishizuka, S., Oba, T., Sakamoto, T., and Koizumi, I.: Eastern Mediterranean surface water temperatures and δ^{18}O composition

during deposition of sapropels in the late Quaternary, Paleoceanography, 18, 5-1-5-17, doi:10.1029/2000PA000617, 2003. 2007
Farmer, D. M. and Armi, L.: Maximal two-layer exchange over a sill and through the combination of a sill and contraction with barotropic flow, J. Fluid. Mech., 164, 53–76, 1986. 2027
Farrera, I., Harrison, S. P., Prentice, I. C., Ramstein, G., Guiot, J., Bartlein, P. J., Bonnefille, R., Bush, M., Cramer, W., von Grafenstein, U., Holmgren, K., Hooghiemstra, H., Hope, G., Jolly, D., Lauritzen, S.-E., Ono, Y., Pinot, S., Stute, M., and Yu, G.: Tropical climates at the Last Glacial Maximum: a new synthesis of terrestrial palaeoclimate data, I. Vegetation, lake-levels and geochemistry, Clim. Dynam., 15, 823–856, 1999. 2018
Hagemann, S. and Dümenil-Gates, L.: An improved sub grid runoff parameterization scheme for climate models, Clim. Dynam., 21, 349–359, 203. 2010
Hayes, A., Kucera, M., Kallel, N., Sbeffi, L., and Rohling, E. J.: Glacial Mediterranean sea surface temperatures based on planktonic foraminiferal assemblages, Quaternary Sci. Rev., 24, 999–1016, 2005. 2007, 2019, 2020, 2021, 2022, 2047, 2049
Jaeger, L.: Monatskartendes Niederschlags für die ganze Erde, Ber. Dtsch. Wetterdienstes, 18, 138, 1976. 2015, 2016
Jerlov, N. G.: Marine Optics, Elsevier Oceanography Series, 14, Elseiver, 231 pp., 1976. 2009
Jost, A., Lunt, D., Kageyama, M., Abe-Ouchi, A., Peyron, O., Valdes, P. J., and Ramstein, G.: High-resolution simulations of the last glacial maximum climate over Europe: a solution to discrepancies with continental palaeoclimatic reconstructions? Clim. Dynam., 24, 577–590, DOI 10.1007/s00382-005-0009-4, 2005. 2018
Kim, S.-J., Crowley, T. J., Erickson, D. J., Govindasamy, B., Duffy, P. B., and Lee, B. Y.: High-resolution climate simulation of the last glacial maximum, Clim. Dynam., 31, 1–16, 2008. 2018
Lee, K. E: Compilation of alkenone LGM SST data, doi:10.1594/PANGAEA.103070, 2004. 2019, 2020, 2047, 2049
Kohfeld, K. E. and Harrison, S. P.: How well can we simulate past climates? Evaluating the models using global palaeoenvironmental datasets, Quaternary Sci. Rev., 19(1–5), 321–346, 2000. 2018
Lacombe, H. and Richez, C.: The regime of the Strait of Gibraltar, in: Hydrodynamics of Semi-Enclosed Seas, edited by: Nihoul, J. C. J., Elsevier, Amsterdam, 13–73, 1982. 2015, 2016
Legates, D. R., and Wilmot, C. J.: Mean seasonal and spatial variability in guage-corrected, global precipitation, Int. J. Climatol., 10, 111–127, 1990. 2016

CPD
6, 2005–2054, 2010

Modeling Mediterranean ocean climate of the LGM

U. Mikolajewicz

Ludwig, W., Dumont, E., Meybeck, M., and Heussner, S.: River discharges of water and nutrients to the Mediterranean and Black Sea: Major drivers for ecosystem changes during past and future decades? Progr. Oceanogr., 80, 199–217, 2009. 2010, 2016

Maier-Reimer, E.: Design of a closed boundary regional model of the Arctic Ocean, Bull. Amer. Meteor. Soc.: Workshop on polar processes in global climate, 13–15 Nov, 1996, 72–73, 1997. 2008

Malmgren, B.A., Kucera, M., Nyberg, J., Waelbroeck, C.: Comparison of statistical and artificial neural networks for estimating past sea surface temperatures from planktonic foraminifer census data, Paleoceanography, 16(5), 520–530, 2001. 2019

Mariotti, A., Struglia, A. V., Zeng, N. and Lau, K.-M.: The Hydrological Cycle in the Mediterranean Region and Implications for the Water Budget of the Mediterranean Sea, J. Climate, 15, 1674–1690, 2002. 2015, 2016

Marsland, S., Haak, H., Jungclaus, J., Latif, M., and Roeske, F.: The Max Planck Institute global ocean/sea ice model with orthogonal curvilinear coordinates, Ocean Model., 5, 91–127, 2003. 2008

Matthiesen, S. and Haines, K.: A hydraulic box model study of the Mediterranean response to postglacial sea-level rise. Paleoceanography, 18(4), 1084, doi:10.1029/2003PA000880, 2003. 2027

MEDAR Group: MEDATLAS/2002 database. Mediterranean and Black Sea database of temperature salinity and bio-chemical parameters, Climatological Atlas, IFREMER Edition (4 Cdroms), 2002. 2011

Mikolajewicz, U. and Maier-Reimer, E.: Mixed boundary conditions in ocean general circulation models and their influence on the stability of the model's conveyor belt, J. Geophys. Res., 99(C11), 22633–22644, 1994. 2025

Mikolajewicz, U., Vizcaino, M., Jungclaus, J., and Schurgers G.: Effect of ice sheet interactions in anthropogenic climate change simulations, Geophys. Res. Lett., 34, L18706, doi:10.1029/2007GL031173, 2007. 2009

Myers, P. G., Haines, K., and Rohling, E. J.: Modelling the paleocirculation of the Mediterranean: The last glacial maximum and the Holocene with emphasis on the formation of sapropel S1, Paleoceanography, 13, 586–606, 1998. 2007, 2024, 2025, 2026, 2030

Peltier, W.R.: Global glacial isostasy and the surface of the ice-age Earth: the ICE-5G (VM2) model and GRACE, Annu. Rev. Earth Pl. Sc., 32, 111–149, 2004. 2009, 2016

Pickard, G. L. and Emery, W. J.:Descriptive physical oceanography, Pergamon Press, Oxford,

CPD

6, 2005–2054, 2010

Modeling Mediterranean ocean climate of the LGM

U. Mikolajewicz

320 pp., 1990. 2014
Pinardi, E. and Masetti, E.: Variability of the large scale general circulation of the Mediterranean Sea from observations and modelling: a review, Palaeogeography, Palaeoclimatology, Palaeoecology, 158, 153–173, 2000. 2015
Reeder, M. S., Stow, D. A. V., and Rothwell, R. G.: Late Quaternary turbidite input into the east Mediterranean basin: new radiocarbon constraints on climate and sea-level control, in: Sediment Flux to Basins: Causes, Controls, and Consequences,edited by: Jones, S. J. and Frostick, L. E., Geological Society of London, Special Publication, 191, 267–278, 2002. 2018
Robinson, S. A., Black, S., Selwood, B. W., and Valdes, P. J.: A review of paleoclimates and paleoenvironments in the Levant and the eastern Mediterranean from 25,000 to 5000 years BP: setting the envoronmental background for the evolution of human civilisation, Quaternary Sci. Rev., 25, 1517–1541, 2006. 2007
Roeckner, E., Bäuml, G., Bonaventura, L., Brokopf, R., Esch, M., Giorgetta, M., Hagemann, S., Kirchner, I., Kornblueh, L., Manzini, E., Rhodin, A., Schlese, U., Schulzweida, U., and Tompkins, A.: The atmospheric general circulation model ECHAM5, Part I: Model description, Max Planck Institute for Meteorology, Hamburg, Report no. 349, 2003. 2009
Rohling, E. J.: Environmental controls on salinity and δ^{18}O in the Mediterranean, Paleoceanography, 14, 706-7-15, 1999. 2026
Rohling, E. J., and Bryden, H. L.: Estimating past changes in the eastern Mediterranean freshwater budget using reconstructions of sea level and hydrography, Proc. K. Ned. Akad. Wet. Biol. Chem. Geol. Phys. Med. Sci., 97, 201–217, 1994. 2007, 2026
Stein, M., Torfstein, A., Gavrieli, I., and Yechieli, Y.: Abrupt aridities and salt deposition in the post-glacial Dead Sea and their North Atlantic connection, Quaternary Sci. Rev., 1–9, doi:10.1016/j.quascirev.2009.10.015, 2009. 2017
Thiede, J.: A Glacial Mediterranean, Nature, 276, 680–683, 1978. 2006, 2022
Thunell, R. C., and Williams, D. F.: Glacial-Holocene salinity changes in the Mediterranean Sea: Hydrographic and depositional effects, Nature, 338, 493–496, 1989. 2007, 2023
Tolmazin, D .: Changing coastal oceanography of the Black Sea I, Northwestern shelf, Prog. Oceanogr., 15, 217–276, 1985. 2016
Vörösmarty, C. J., Fekete, B. M., and Tucker, B. A.: Global River Discharge 18071991, RivDIS v1.1. Available from: http://www.daacsti.ornl.gov//RIVDIS/guides/rivdis_guide.html. Last update: June 2004, 1998. 2010

Waelbroeck, C., Labeyrie, L., Duplessy, J., Guiot, J., Labracherie, M., Leclaire, H., and Duprat, J.: Improving past sea surface temperature estimates based on planktonic fossil faunas, Paleoceanography 13(3), 272–283, 1998. 2019

WOA: World Ocean Atlas 1998, Version 2, http://www.nodc.-noaa.gov/oc5/woa98.html. Tech. rep., NationalOceanographic Data Center, Silver Spring, Maryland, 1998. 2020

Wu, H., Guiot, J., Brewer, S., and Guo, Z.: Climatic changes in Eurasia and Africa at the Last Glacial Maximum and mid-Holocene: reconstruction from pollen data using inverse vegetation modelling, Clim. Dynam., 29, 211–229, 2007. 2017, 2018

Xie, P. and Arkin, P. A.: Global monthly precipitation estimates from satellite-observed outgoing longwave radiation, J. Climate, 11, 137–164, 1998. 2016

Table 1. Hydrological budget of the Mediterranean. Numbers are given in 1000 $m^3 s^{-1}$ unless specified explicitely on top of the column. Numbers in $m\,yr^{-1}$ are basin averaged fluxes.

	CTL Mediterranean		CTL Black Sea	CTL total	LGM Mediterranean	
		$m\,yr^{-1}$				$m\,yr^{-1}$
precipitation	32.1	0.39	7.9	39.9	30.4	0.43
evapaporation	−97.3	−1.19	−12.7	−110.0	−77.9	1.10
river runoff	11.3		11.7	23.0	19.3	
net flux	−54.0	−0.66	6.9	−47.1	−28.2	−0.40

CPD

6, 2005–2054, 2010

Modeling Mediterranean ocean climate of the LGM

U. Mikolajewicz

Table 2. Annual mean basin average heat fluxes for the Mediterranean in W/m^2.

	CTL	LGM
absorbed shortwave radiation	168.2	169.3
net longwave radiation	−68.1	−73.1
latent heat flux	−96.4	−89.5
sensible heat flux	−7.7	−11.2
total	4.0	4.5

CPD
6, 2005–2054, 2010

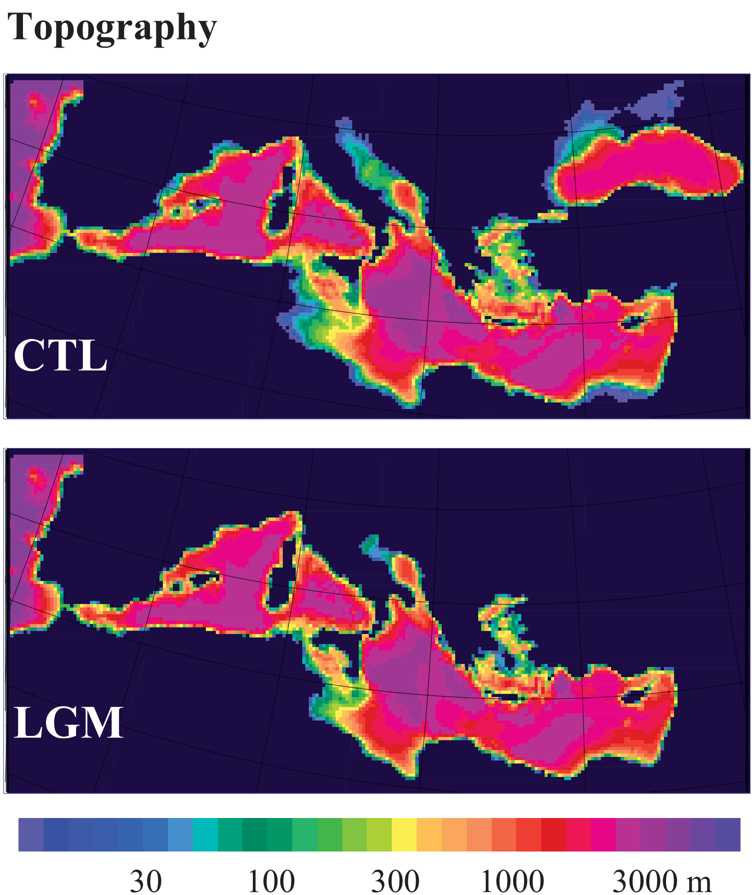

Fig. 1. Model topography in m for CTL (top) and LGM (bottom). Geographical coordinates are drawn for every 10° in longitude and 5° in latitude.

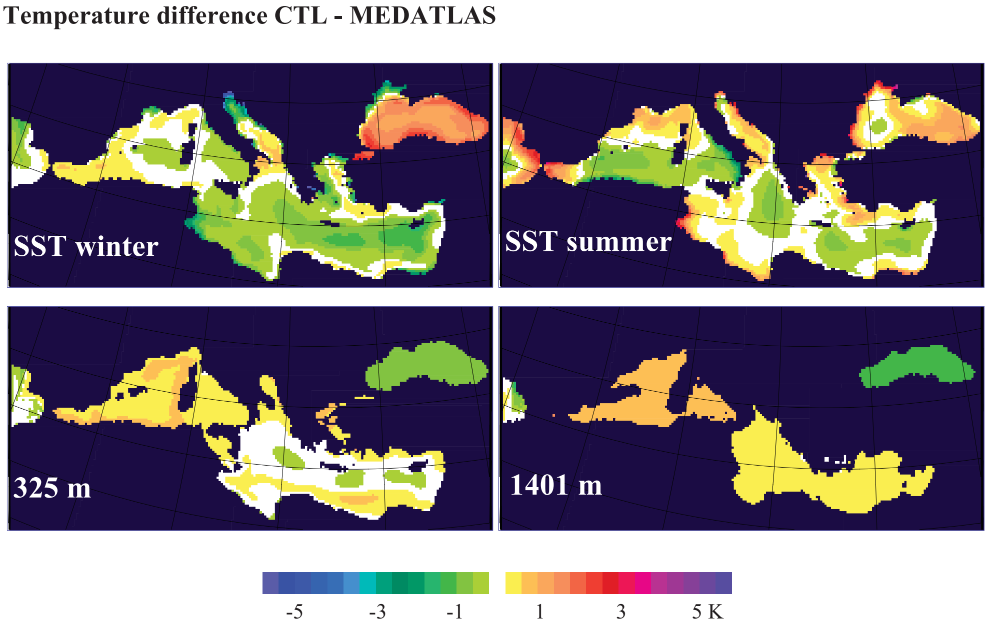

Fig. 2. Difference between simulated (CTL) and climatological (MEDATLAS) potential temperatures in K. Winter (JFM) and summer (JAS) SST and annual mean temperatures at 325 m and 1401 m depth. Contour interval is 0.4 K. White indicates deviations smaller than 0.2 K.

CPD
6, 2005–2054, 2010

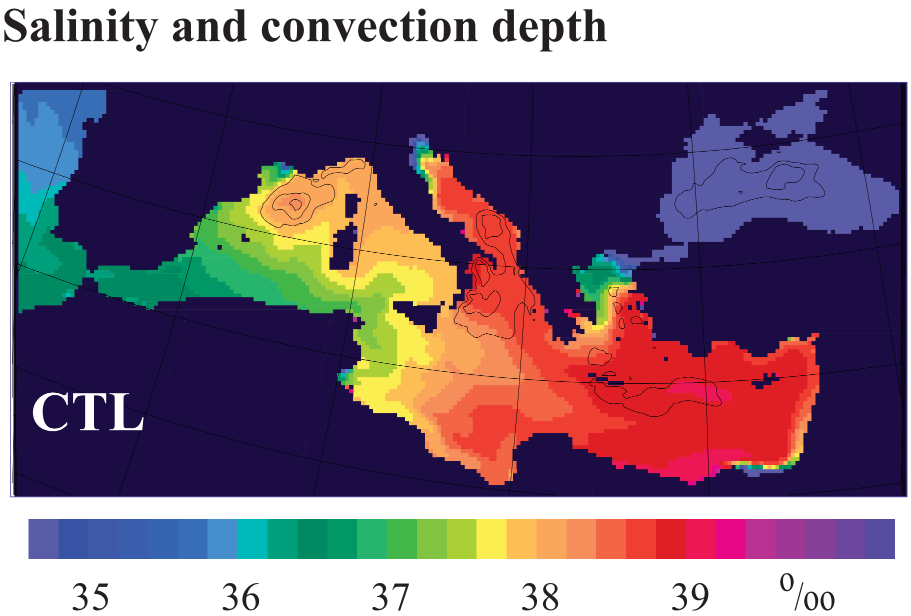

Fig. 3. The colours show the simulated annual mean surface salinity in CTL in ‰. Contour interval is 0.2‰. Isolines show the climatological maximum depth of the mixed layer. Contour interval is 250 m.

CPD
6, 2005–2054, 2010

Modeling Mediterranean ocean climate of the LGM

U. Mikolajewicz

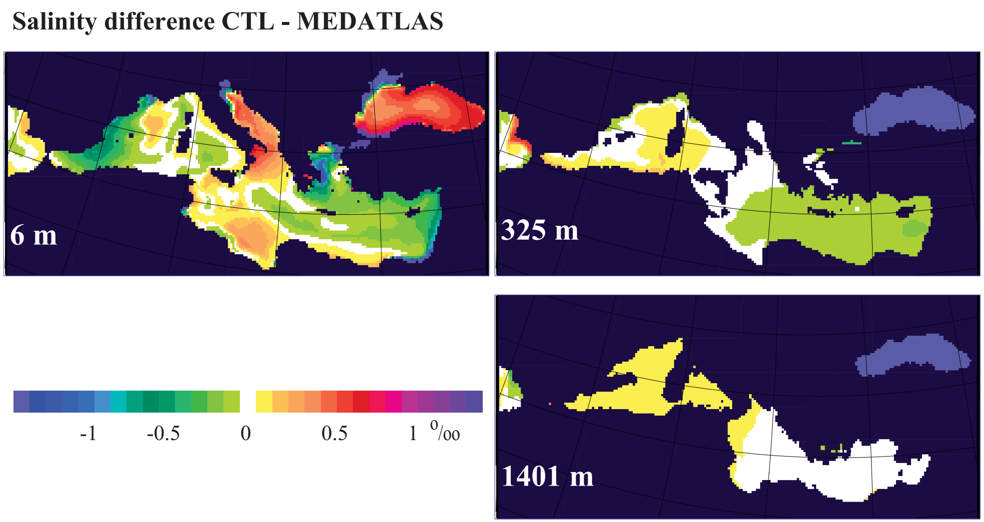

Fig. 4. Difference between simulated (CTL) and climatological annual mean salinity (MEDATLAS) for the surface, 325 m and 1401 m. Contour interval is 0.1‰. White indicates deviations smaller than 0.05‰.

CPD
6, 2005–2054, 2010

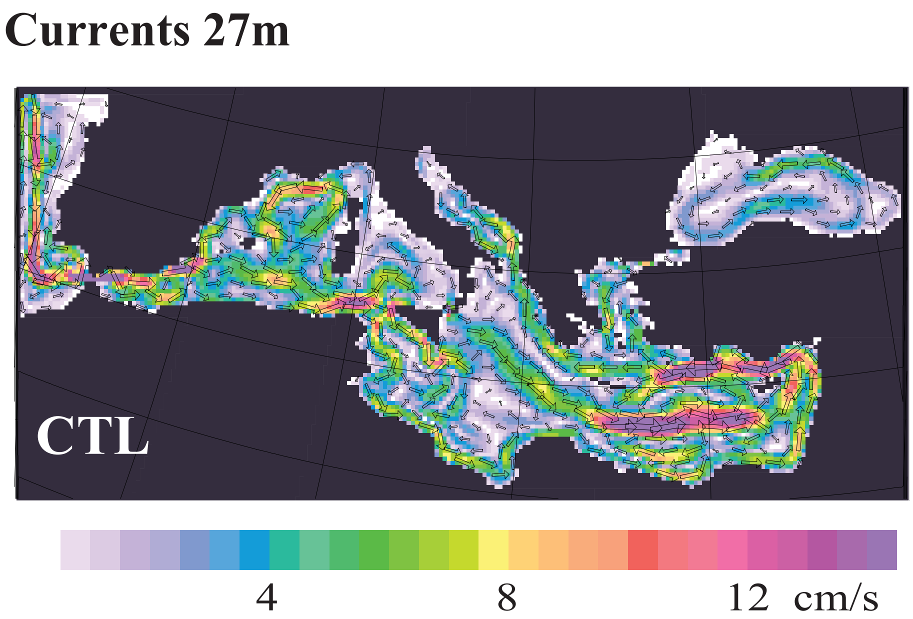

Fig. 5. Currents at 27 m depth for CTL. Colours indicate the flow speed in $cm s^{-1}$, vectors both direction and speed. Only a subset of vectors has been plotted.

CPD
6, 2005–2054, 2010

Modeling Mediterranean ocean climate of the LGM

U. Mikolajewicz

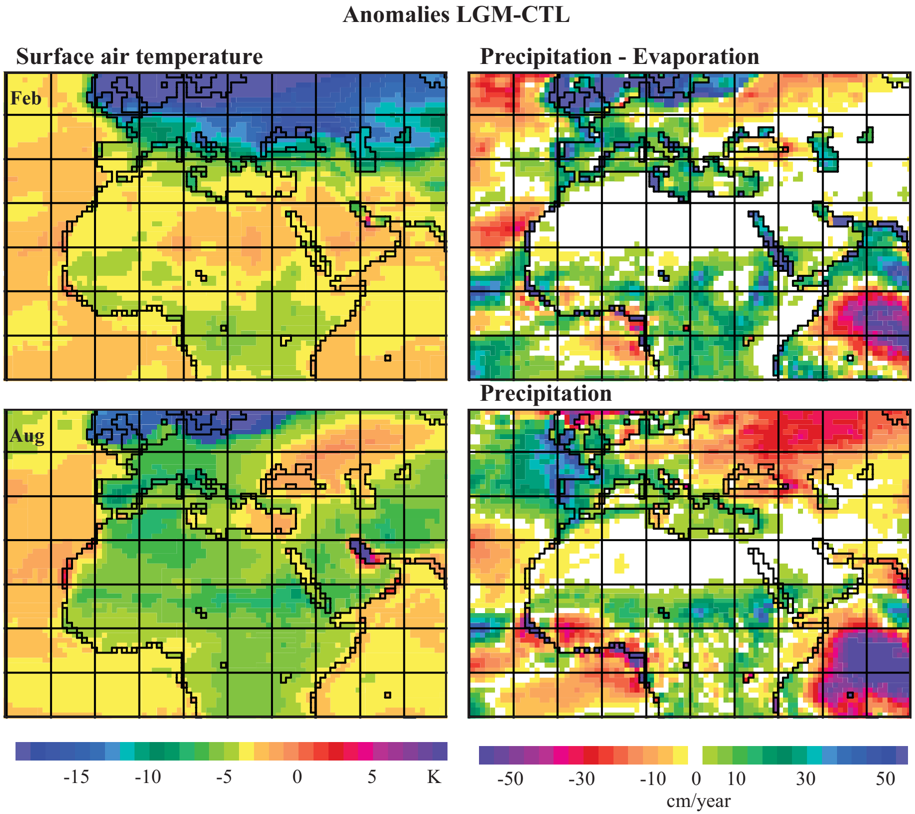

Fig. 6. Left: Difference between LGM and present day simulations with the stand-alone ECHAM5 T106 atmospheric model. Left: Difference in surface air temperature between LGM and present day in K for February (top) and August (bottom). Right: Difference in annual mean precipitation minus evaporation (top) and precipitation (bottom). Contour interval is 4 cm/yr, white colour indicates changes less than 2 cm/yr. Both present day and LGM coastlines are shown.

CPD
6, 2005–2054, 2010

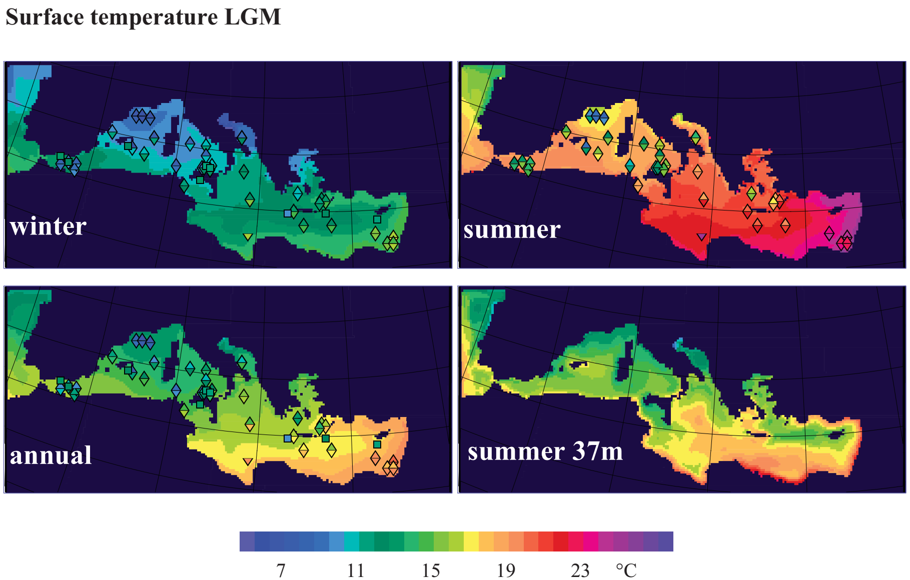

Fig. 7. Simulated temperature in the LGM simulation in °C. Winter (JFM) SST, annual mean SST, summer (JAS) SST and summer temperature at 37 m depth. Downward triangles represent ANN reconstructions, upward looking triangles represent RAM reconstructions (Hayes et al., 2005). Alkenone derived temperature estimates (Lee, 2004) are represented by squares. Extending the suggestion by Emeis et al. (2000), alkenone temperature estimates have also been plotted for winter.

CPD
6, 2005–2054, 2010

Modeling Mediterranean ocean climate of the LGM

U. Mikolajewicz

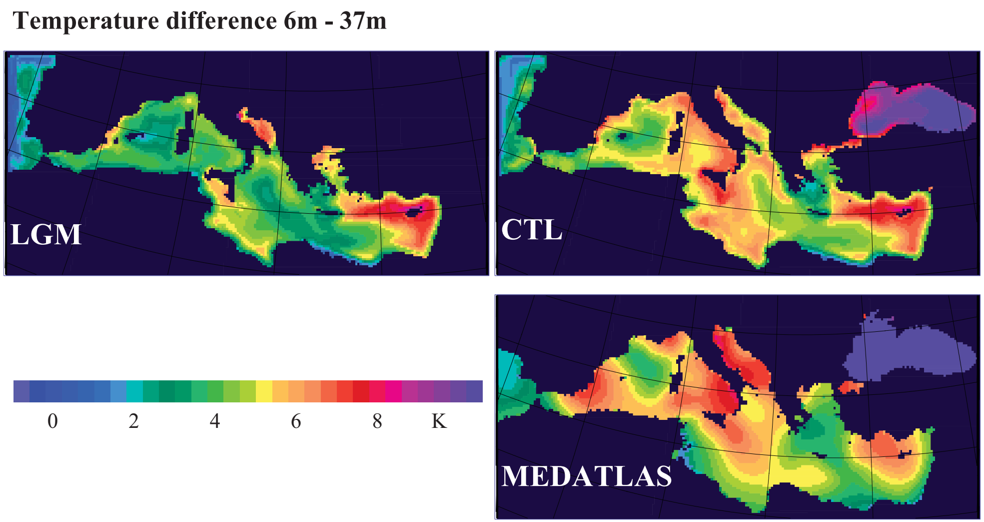

Fig. 8. Differences between summer (JAS) temperatures at 6 and 37 m in K. LGM, CTL and observations (MEDATLAS).

CPD
6, 2005–2054, 2010

Modeling Mediterranean ocean climate of the LGM

U. Mikolajewicz

Surface temperature anomaly

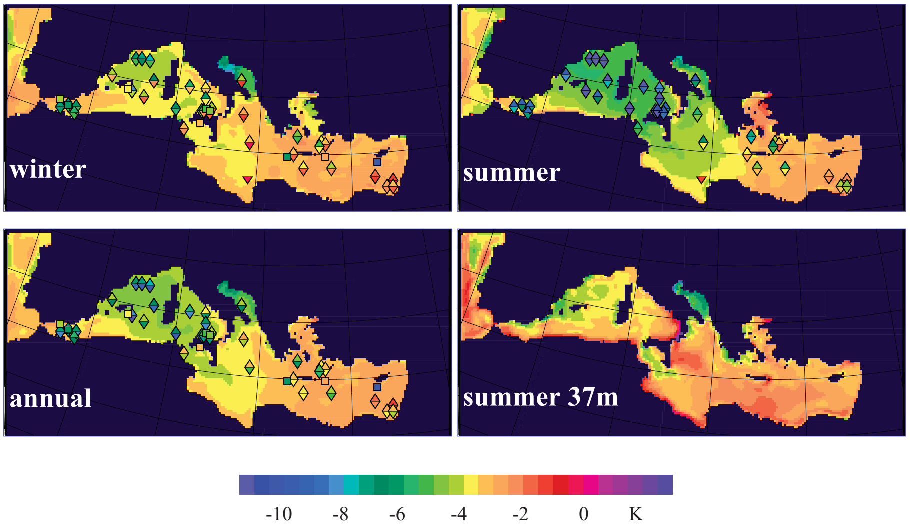

Fig. 9. Simuated temperature anomalies between LGM and CTL in K. Winter (JFM) SST, annual mean SST, summer (JAS) SST, and summer temperature anomalies at 37 m depth. Triangles represent anomalies between SST recontructions from assemblages of foraminifera (Hayes et al., 2005) and WOA98 temperatures at 10 m depth. Downward triangles represent reconstruction using the ANN method, upward looking triangles using the RAM method. Squares represent differences between alkenone derived temperature estimates for LGM and core top (Lee, 2004).

CPD
6, 2005–2054, 2010

Modeling Mediterranean ocean climate of the LGM

U. Mikolajewicz

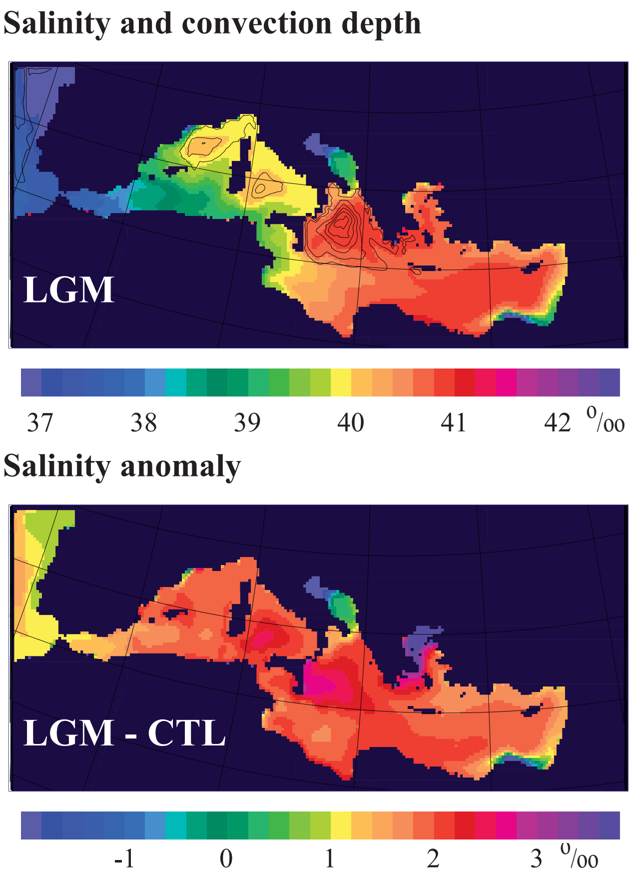

Fig. 10. Top: Simulated annual mean surface salinity (colours, contour interval 0.2‰) and climatological maximum mixed layer depth (isolines, contour interval 250 m) for LGM. For CTL see Fig. 3. Bottom: Anomalies of surface salinity LGM minus CTL wth a contour interval of 0.2‰.

CPD
6, 2005–2054, 2010

Modeling Mediterranean ocean climate of the LGM

U. Mikolajewicz

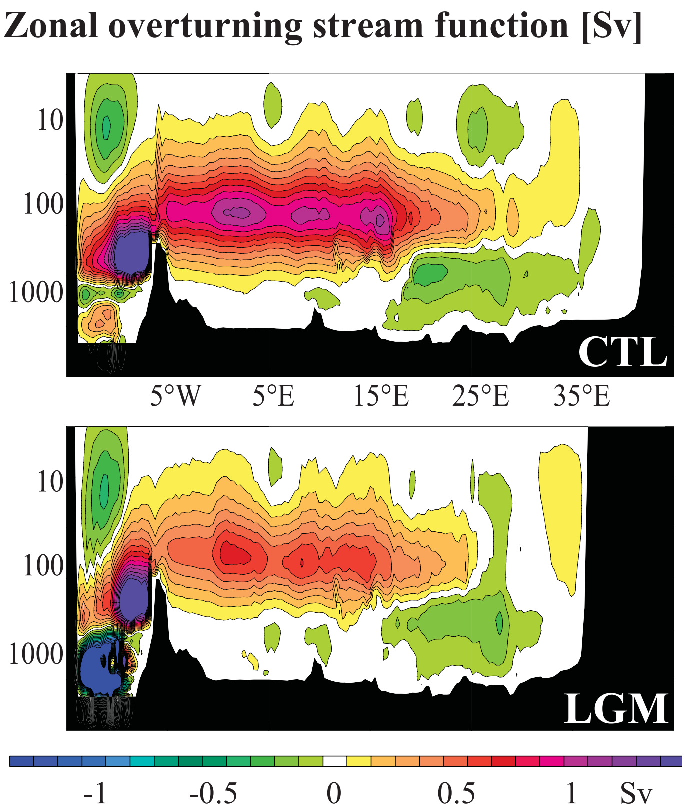

Fig. 11. Meridionally integrated zonal overturning stream function in Sv. Positive values indicate clockwise circulation. The y-axis shows depth in m on a logarhythmic scale vs. longitude. The top panel shows CTL, the bottom panel LGM. Contour value is 0.1 Sv, white indicates values smaller than ±0.05 Sv.

CPD
6, 2005–2054, 2010

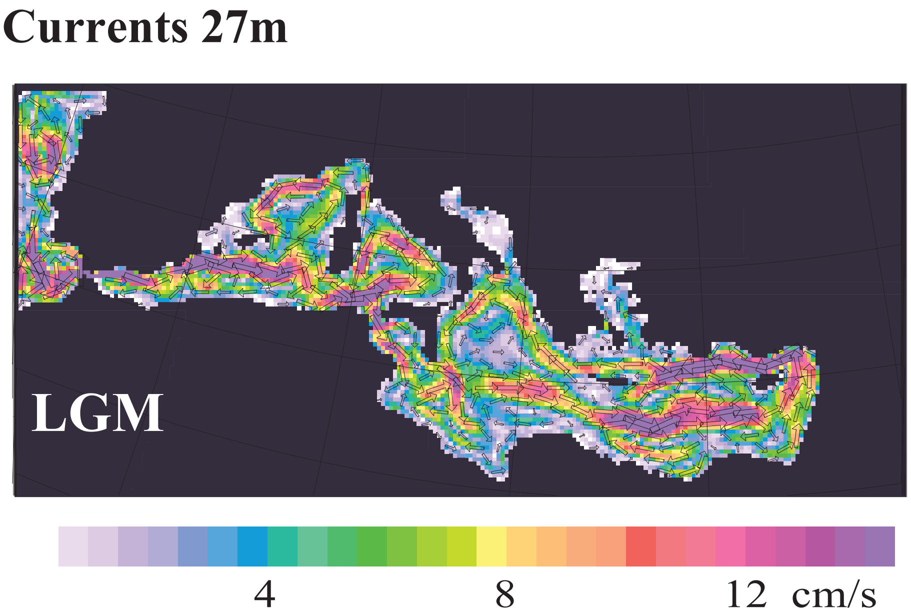

Fig. 12. Currents at 27 m depth for LGM. Colours indicate the flow speed in $cm s^{-1}$, vectors both direction and speed. Only a subset of vectors has been plotted. For CTL see Fig. 5

CPD
6, 2005–2054, 2010

CPD
6, 2005–2054, 2010

Modeling Mediterranean ocean climate of the LGM

U. Mikolajewicz

Title Page
Abstract | Introduction
Conclusions | References
Tables | Figures
◂◂ | ▸▸
◂ | ▸
Back | Close
Full Screen / Esc
Printer-friendly Version
Interactive Discussion

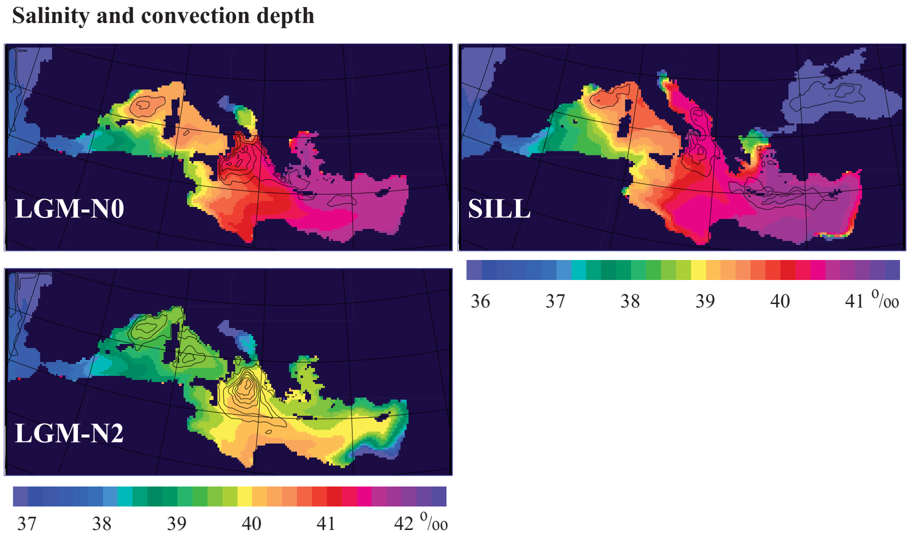

Fig. 13. Simulated annual mean surface salinity (colours, contour interval 0.2‰) and climatological maximum mixed layer depth (isolines, contour interval 250 m) for sensitivity experiments. The panels on the left show the LGM experiments with modified Nile discharge: Suppressed (LGM-N0) and doubled (LGM-N2) Nile discharge. The right panel shows the results for the present day sensitivity experiment with reduced sill depths in the Straits of Gibraltar and Sicily. Cw. Figs. 10top and 3.

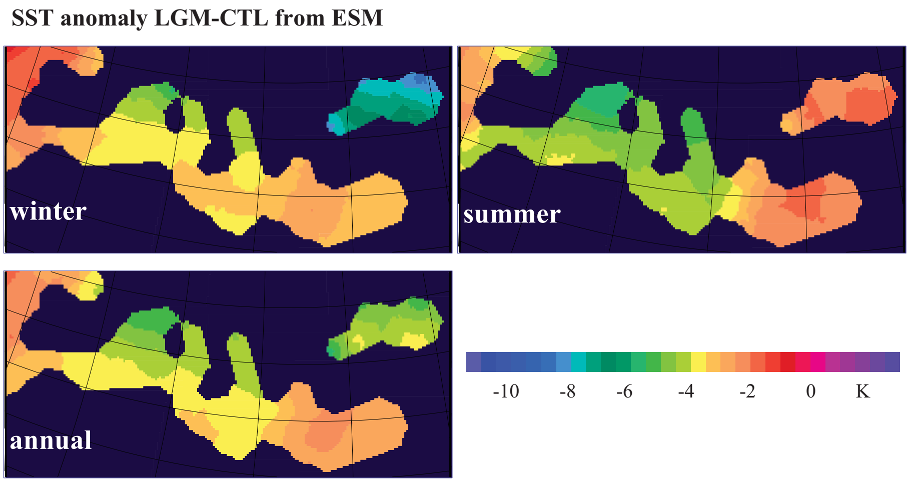

Fig. 14. Simuated SST anomalies LGM-CTL from the ESM in K. Winter (JFM), annual, and summer (JAS). The data have been interpolated onto the grid of the regional model. Cw. Fig. 9. The land sea mask has been interpolated from the ocean component of the ESM.

CPD
6, 2005–2054, 2010

Modeling Mediterranean ocean climate of the LGM

U. Mikolajewicz